Polymer Nanocomposites Based on Needle-like Sepiolite Clays: Effect of Functionalized Polymers on the Dispersion of Nanofiller, Crystallinity, and Mechanical Properties

E. Bilotti,[1] H. R. Fischer,[2] T. Peijs[1,3]

[1]*Department of Materials, Queen Mary, University of London, Mile End Road E1 4NS, London, United Kingdom*
[2]*TNO-TPD, Innovative Materials, P. O. Box 595, 5600 AN Eindhoven, The Netherlands*
[3]*Eindhoven University of Technology, Eindhoven Polymer Laboratories, P. O. Box 513, 5600 MB Eindhoven, The Netherlands*

Received 3 February 2006; accepted 31 July 2006
DOI 10.1002/app.25395
Published online 9 October 2007 in Wiley InterScience (www.interscience.wiley.com).

ABSTRACT: Polypropylene (PP)/sepiolite (Sep) nanocomposites are prepared by melt compounding in a mini-extruder apparatus. The often used maleic anhydride-modified polypropylene (PP-g-MA) is compared with two custom-made functionalized polymers, PP-acid and the di-block copolymer PP-PEO, with respect to the filler dispersion and filler reinforcement efficiency. For that purpose, morphological and mechanical studies are carried out by means of scanning electron microscopy (SEM), transmission electron microscopy (TEM), and mechanical tensile tests. In addition, the nanocomposites are characterized by wide-angle X-ray scattering (WAXS) and differential scanning calorimetric (DSC) techniques, to assess the effect of the nanofiller on the crystalline structure of the PP matrix nano-filler. The use of PP-PEO and PP-acid resulted in a better nanofiller dispersion compared with traditional PP-g-MA-modified systems. Sepiolite acts as nucleating agent for the crystallization of PP and seems to lead to an orientation of the α-phase crystals. © 2007 Wiley Periodicals, Inc. J Appl Polym Sci 107: 1116–1123, 2008

Key words: polypropylene; nanoclay; sepiolite; nanocomposites

INTRODUCTION

Polymer–clay nanocomposite materials have attracted considerable interest since the pioneering work carried out by Toyota Central Research Laboratories on Nylon 6-Montmorillonite (MMT) nanocomposites, obtained by an in situ polymerization method,[1] and the first fundamental studies by Giannelis and co-workers.[2–5] The result of these experiments demonstrated the possibility of improving significantly the Young's modulus and heat distortion temperature at low nanofiller content without compromising tensile strength, impact strength, or optical transparency significantly. Following up on the initial success of PA-6-based nanocomposites, a wide range of polymers have been evaluated. For an overview of clay containing polymer nanocomposites, the reader is referred to several review papers.[2,6–8]

Nanocomposites based on isotactic polypropylene (iPP) have been studied extensively because of the industrial importance of this polymer. In early studies, Kato and colleagues[9–11] described the melt intercalation of PP modified with either maleic anhydride (PP-g-MA) or hydroxyl groups (PP-OH) in octadecylammonium-exchanged MMT. Mulhaupt and colleagues[12] carried out a systematic study on synthetic hectorite, cation exchange reacted with several protonated primary alkyl amines, and melt compounded in PP together with two different PP-g-MA grades. More recently, Manias et al.[13] published a general review on the properties of PP-based nanocomposites.

So far, most of the research reported in the literature on clay nanocomposites has focused on platelet-like clays, such as MMT. In the present study, we have investigated nanocomposites based on Sepiolite,[14–16] a needle-like-shaped nanoclay. It is believed that this fibrous nanofiller can be more easily dispersed in polymeric matrices because of its lower specific surface area compared with platelet-like clays of the same aspect ratio. The relatively small contact surface and hence the reduced tendencies to agglomerate, could then lead to a better mechanical reinforcement of needle-like clays.[17] Sepiolite is a hydrated magnesium silicate and is part of the phyllosilicate mineral family. It is formed of blocks structurally similar to layered clay minerals (i.e., MMT), composed of two tetrahedral silica sheets and a central octahedral sheet containing Mg, but continuous only in one direction (c-axis) (Fig. 1). More blocks are

Correspondence to: T. Peijs (t.peij@qmul.ac.uk).
Contract grant sponsor: STRP (European Research Program NANOFIRE, Sixth Framework Program); contract grant number: 505637.

Journal of Applied Polymer Science, Vol. 107, 1116–1123 (2008)

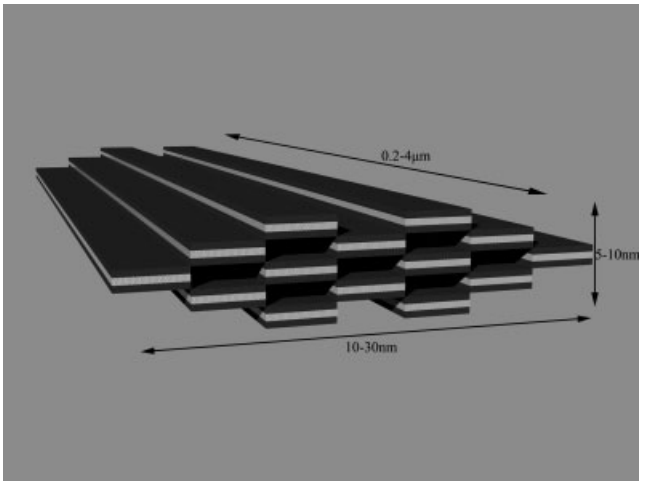

Figure 1 Schematic illustration of sepiolite fiber with characteristic average sizes, showing blocks and channels extending in the longitudinal direction. Each block is formed by two tetrahedral silica sheets and a central octahedral sheet containing Mg, represented by a dark and light colors, respectively. More blocks are structurally linked to each others along their longitudinal edges by Si—O—Si bonds.

linked together along their longitudinal edges by Si—O—Si bonds, and this creates channels along the c-axis. Because of the discontinuity of the external silica sheets, a significant number of silanol groups (SiOH) are situated at the edges of this mineral.[18,19] Sepiolite shows high surface areas, $\sim$ 200–300 m^2/g, due to its fine particle size and fibrous nature, but also to the presence of channels and micropores.[20] The dimensions of the fibers vary between 0.2– 4 μm in length, 10–30 nm in width, and 5–10 nm in thickness. Sepiolite is naturally found in bundles due to the attraction forces.

The fundamental concept of nanocomposites is based on the high aspect ratios and large interfaces provided by the nanofillers and hence a substantial reinforcement achieved at small loadings. However, the peculiarity of nanofillers to have very high specific surface areas and small dimensions simultaneously leads to a preference for agglomeration in micrometric stacks or bundles due to van der Waals interactions, ionic interaction, and/or hydrogen bonds. Therefore, the ability to control the dispersion of nanofillers in a polymeric phase is the key issue that affects the performance of the final material and the possibility itself to obtain nanocomposite. The use of a modified polymer as a third phase in nanocomposite systems could be an effective way to promote the dispersion of the nanofiller.[21,22] We know that it is possible to modify the properties of interfaces; for instance, we can reduce the surface energy of a polymer melt by blending in a polymer of lower surface energy that segregates to the surface and that can be adsorbed to the interface of solid particles, whose properties would thereby be modified. The adsorbed polymer can decrease the surface energy of the particles and therefore their interactions. The basic idea of a surface-active polymer is the same as that for small-molecule surfactant: we use a molecule in which various parts of the molecule have different affinities with the various parts of the interface. In this study, we compared three surface-active polymers: PP grafted maleic anhydride (PP-g-MA), a functionalized PP-acid, and the di-block copolymer PP-PEO, with respect to the filler dispersion and filler reinforcement efficiency. These three polymers are characterized by the presence of different functional groups and hence different affinities with the filler surface, but also by different molecular weights. The nanocomposites morphology will result to change substantially in relation to the surface-active polymer employed.

Another important issue in nanocomposites is the variation of properties of the polymer matrix induced by nanofillers. In fact, semi-crystalline polymers, like iPP, can be relevantly affected in their crystalline structure as well as in their total crystallinity, as a consequence of the presence of fillers[23–26], and that can result in differences in properties.

The most important effect of particulate fillers is their ability to act as nucleating agents. The very strong nucleating effect of talc, for example, has been widely demonstrated.[27,28] The influence of other fillers is often not so clear. $CaCO_3$, for instance, has been frequently classified as inactive filler. However, a significant increase in the nucleating effect of $CaCO_3$ was observed with decreasing particle size and, as a consequence, increasing particle aggregation.[29] The nucleation effect of MMT was also studied in melt blended iPP nanocomposites.[30–32] Pozsgay et al.[31] demonstrated that the ability of MMT to nucleate iPP depends on organo-treatment of clay and, hence, on the alteration of interlayer MMT distance rather than on the modification of the clay surface tension. These investigators concluded that the nucleation occurs not on the surfaces, but rather in the interlayers, of clay particles and attributed the nucleating effect to the collapsed MMT galleries of 1-nm distance. Svoboda et al.[32] found an increase in crystallization temperatures in PP-g-MA/MMT systems containing clay tactoids, but not in systems with well-dispersed MMT clays.

Next to changing the overall crystallinity, the presence of a filler material can also modify the crystal structure of a semi-crystalline polymer. For instance, it is known that iPP is able to crystallize in different polymorphic forms: α, β, γ, and a mesomorphic crystal structure.[33,34] The α, or monoclinic, form is the most predominant in melt crystallized PP. The β, or hexagonal, form is only present in small amounts, unless specific heterogeneous nucleating agents are employed. Crystallization of iPP in the γ, or triclinic, form strongly depends on specific aspects of the molecular structure. For example, γ phase has been observed in low-molecular-weight, stereo block fractions that have been crystallized at elevated pressure.

To be able to analyze and compare the performance of nanocomposites and the real reinforcing efficiency of the nanofiller, it is essential to investigate how the Sepiolite influences the structure of the polypropylene matrix. Therefore, in addition to microscopy and mechanical experiments, differential scanning calorimetric (DSC) and wide-angle X-ray scattering (WAXS) investigations have been carried out and will be presented in this study.

EXPERIMENTAL

Materials

The i-PP used was Moplen® HP500H (MFR 1.8 g/s 10 min at 230°C/2.16 kg) from Basell (Ferrera, Italy) and the sepiolite Pangel® were supplied by Tolsa (Madrid, Spain). The bulk density of that clay is 60 ± 30 g/L, and the BET surface area is 320 m^2/g. The characteristic averaged dimensions of the individual sepiolite fibers are 1–2 μm in length and 20–30 nm in diameter. So the aspect ratio is within the range of 100–300. The PP-g-MA used is a commercial-grade VINBOND® P series (VB100; 1% grafted MA; MFR 6.0 g/min at 230°C/2.16 kg; $M_w = 151$ kg/mol) from Vin Enterprise, Ltd. PP-PEO and PP-acid are customer-made products from Baker Petrolite (NewYork). The first is a di-block copolymer of $M_n = 1200$ g/mol with a 20–40 wt % of PEO blocks. The second is a carboxylic acid terminated PP of $M_n = 1800$ g/mol, with an acid number of 30.

Preparation of nanocomposites

Nanocomposites were prepared by a two-steps blending process in a mini twin-screw extruder DSM Micro 15 at 200°C for 10 min at 200 rpm. First, Sepiolite was mixed with the functionalized polymer (1 : 1 weight ratio) and PP homopolymer to make a master batch at 10 wt % of filler, which was subsequently diluted with neat PP homopolymer to obtain nanofiller concentrations of 1, 2.5, and 5 wt %. The composition of materials studied is listed in Table I.

Characterization of nanocomposites

Morphological studies were carried out using scanning electron microscopy (SEM) analysis (Jeol JSM-6300F) on gold-coated, cold fractured surfaces and transmission electron microscopy (TEM) analysis (Jeol JEM 2010 TEM) on ultra-thin samples obtained with a microtome.

Tensile tests were conducted in a universal testing machine (Instron 5584), equipped with a 1-kN load cell, standard grips and Merlin software, according to the standard ASTM D-638. The test specimens were dog-bone shaped with a length of 60 mm and a thickness of 1 mm, according to the type V dimensions indicated by the same standard. Specimens were obtained by compression molding at 220°C for 10 min.

TABLE I
Nanocomposites Composition

	Sepiolite	PP-PEO	PP-acid	PP-g-MA
PP+1%Sep	1	—	—	—
PP+2.5%Sep	2.5	—	—	—
PP+5%Sep	5	—	—	—
PP+PP-PEO+1%Sep	1	1	—	—
PP+PP-PEO+2.5%Sep	2.5	2.5	—	—
PP+PP-PEO+5%Sep	5	5	—	—
PP+PP-acid+1%Sep	1	—	1	—
PP+PP-acid+2.5%Sep	2.5	—	2.5	—
PP+PP-acid+5%Sep	5	—	5	—
PP+PP-g-MA+1%Sep	1	—	—	1
PP+PP-g-MA+2.5%Sep	2.5	—	—	2.5
PP+PP-g-MA+5%Sep	5	—	—	5

WAXS spectra were recorded with a Siemens Diffractometer D5000, where the X-ray beam was Ni-filtered CuKα (λ = 1.5405 Å) and radiation operated at 40 kV with a filament current of 40 mA. Corresponding data were collected from 5 to 30° at a scanning rate of 0.01°/min. The samples analyzed were film of thickness 100 μm, hot pressed at 220°C for 10 min.

Nonisothermal crystallization analyses were performed with a DSC TA Q1000. All samples (2.0 ± 0.1 mg) were first heated to 220°C and kept at that temperature for 5min to remove any thermal history and then cooled at a rate of 10°C/min.

RESULTS AND DISCUSSION

Morphological analysis

As mentioned earlier, the dispersion of the nanofiller in the polymer matrix is a crucial aspect for the performance of nanocomposites. SEMs of cold fractured surfaces of different nanocomposite systems are shown in Figure 2 and will be discussed in particular concerning the influence of the different functionalized polymers on the sepiolite dispersion. Figure 2(a) presents a micrograph of PP+Sep nanocomposite with filler concentration of 2.5 wt %. The system is characterized by micrometer sized clusters of sepiolite which will act as inclusions in a nearly filler-free polymeric matrix. Only a minor improvement in dispersion can be observed in case PP-g-MA is employed as surface-active polymer [Fig. 2(b)]. Sepiolite nanofibers are again found mainly in the form of clusters, which are inhomogeneously distributed within the polymer matrix. Instead, the morphology of nanocomposites shown in Figure 2(c) and (d appears significantly different. In these systems, the use of PP-PEO and PP-acid leads to much finer filler dispersion in the polymeric matrix, where aggregates of Sepiolite are no longer evident.

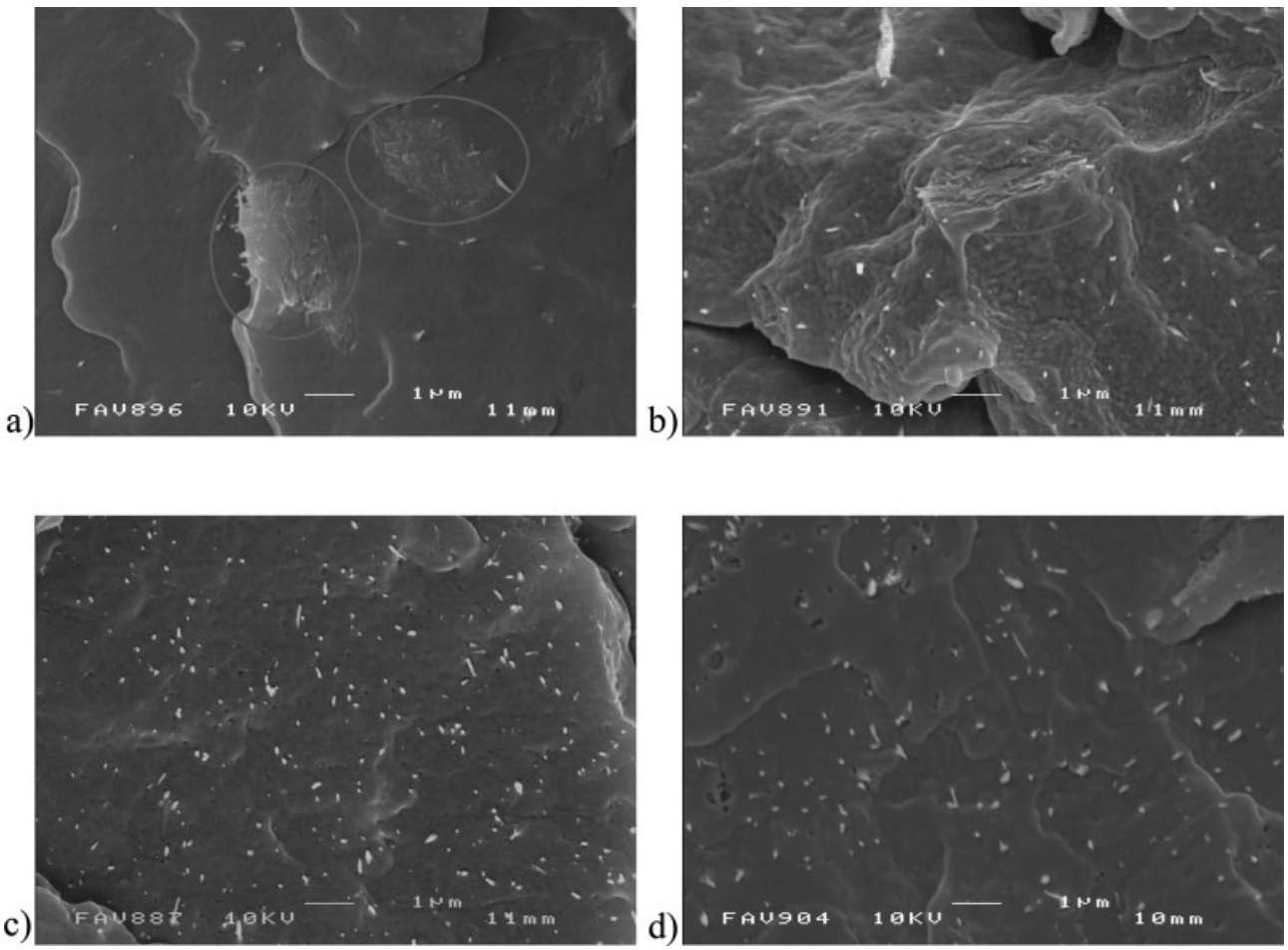

Figure 2 SEMs of: (a) PP+2.5%Sep; (b) PP+PP-g-MA+2.5%Sep; (c) PP+PP-acid+2.5%Sep; (d) PP+PP-PEO+2.5%Sep. Red circles underline Sepiolite clusters. A significant improvement in the dispersion of sepiolite in PP matrix is evident with the use of PP-PEO and PP-acid, where no agglomerates of sepiolite are found in nanocomposites at 2.5 wt % filler load. [Color figure can be viewed in the online issue, which is available at www.interscience.wiley.com.]

The morphology of the nanocomposites has also been investigated by TEM. This analysis, besides confirming the SEM observations, underlines a characteristic fracturing of the sepiolite fibers as a consequence of the mechanical stress during the compounding process. As can be seen in Figure 3(a,b), a reduction of fiber length is evident in the processed nanocomposites compared with the original sepiolite. The length of the fibers is reduced significantly, and the aspect ratio has dropped by almost one order of magnitude, limiting the potential reinforcement of the filler. This aspect will be more deeply studied in future work as preventing the breaking of the sepiolite nanofibers is essential in order to fully exploit the potential of these nanofillers.

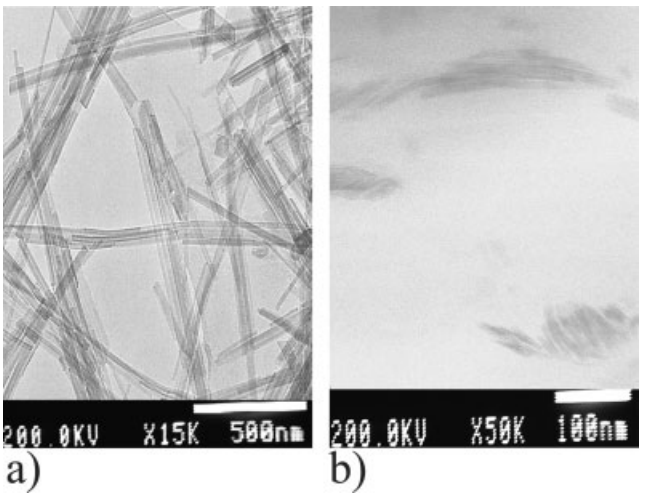

Figure 3 TEM of: (a) Sepiolite powder, and (b) Sepiolite in PP matrix after compounding. A reduction of almost one order of magnitude in fiber length is evident in the processed nanocomposites as a consequence of melt blending in mini-extruder.

Crystal structure and crystallization behavior

Figure 4(a–d) shows the WAXS patterns of sepiolite, PP, and nanocomposites at different filler concentrations. We can see that the sepiolite spectra has a

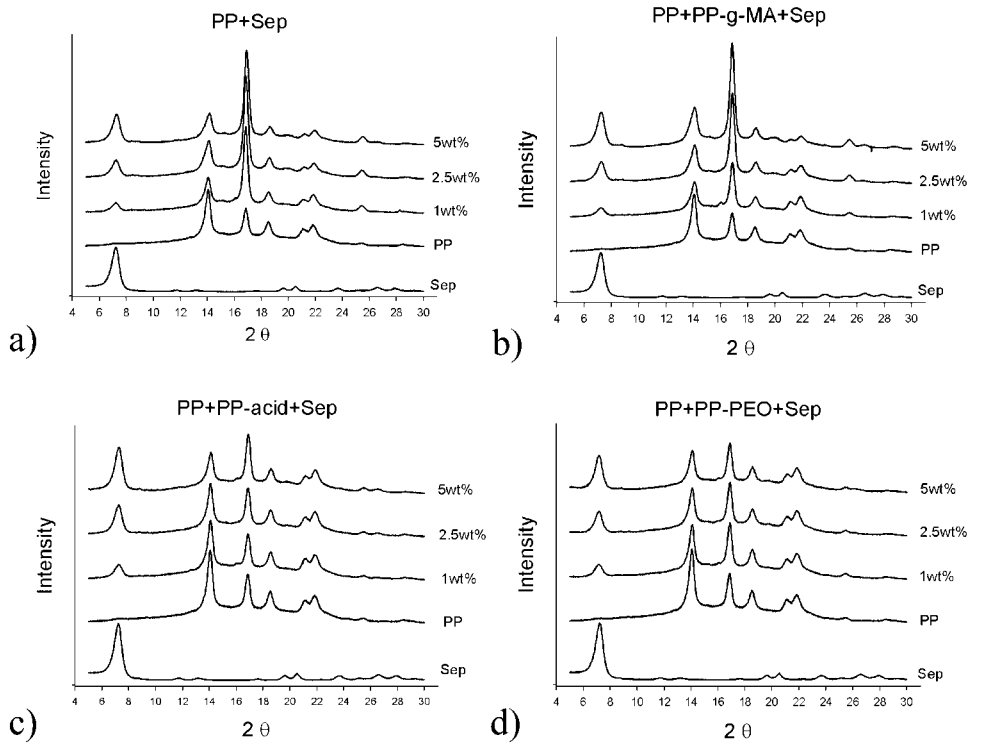

Figure 4 X-ray diffraction spectra of: (a) PP+Sep; (b) PP+PP-g-MA+Sep; (c) PP+PP-acid+Sep; (d) PP+PP-PEO+Sep nanocomposites at different concentrations of filler, compared with virgin PP and pure Sepiolite.

prominent peak at $2\theta = 7.2^\circ$, which corresponds to the primary diffraction of the (100) crystalline plane. The pattern of pure PP shows five main peaks, in the 2θ range of 10–30°, characteristic of the monoclinic α form.[33] For the system PP+Sep [Fig. 4(a)], we can observe that (except for a reflection at $2\theta = 7.2^\circ$, which is typical of Sepiolite), at increasing filler concentrations the same peaks of iPP are observed, suggesting that mainly α-form is present. In particular, there is no evidence of reflections at $2\theta = 16^\circ$, which corresponds to the (300) plane of the β-phase, and at $2\theta = 20.3^\circ$ corresponding to the characteristic (117) plane of the γ-phase. An interesting feature lies in the relative intensities of α-phase peaks. The intensity of the peak at $2\theta = 17^\circ$, which corresponds to the (040) plane of α-phase, increases with filler concentration while the peak at $2\theta = 14^\circ$, corresponding to the (110) plane of α-phase, decreases. This can indicate a preferential orientation of PP crystals induced by the nanofiller, with (040) planes parallel to the specimen surface and the b-axes perpendicular to it.[35–37] The same conclusion may be drawn for the system PP+PP-g-MA+Sep in Figure 4(b). A different situation is observed when PP-acid and PP-PEO are employed [Fig. 4(c,d)], where there is no evidence of a similar orientation enhanced by the nanofiller.

The DSC traces presented in Figure 5 clearly show an increase of the crystallization temperature (T_c), implying that the sepiolite acts as a nucleating agent for the crystallization of polypropylene. Although the

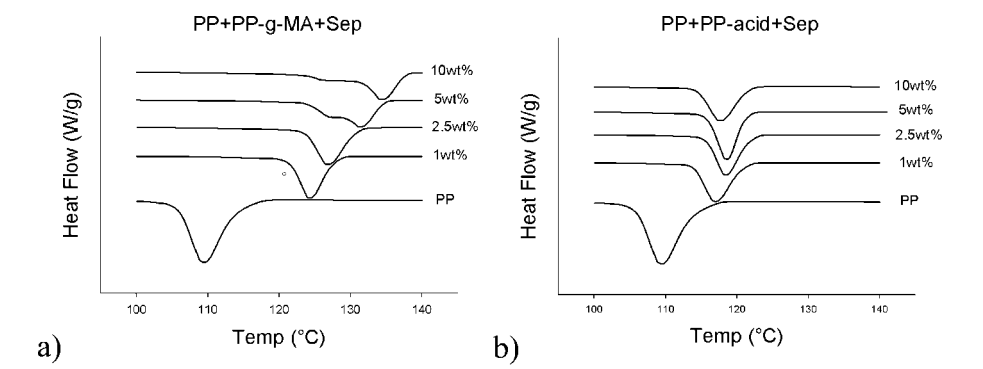

Figure 5 DSC traces corresponding to the nonisothermal crystallization of (a) PP+PP-g-MA+Sep; and (b) PP+PP-acid+Sep at different filler content. The exothermic peaks shift toward higher temperature as a result of the nucleating effect of Sepiolite.

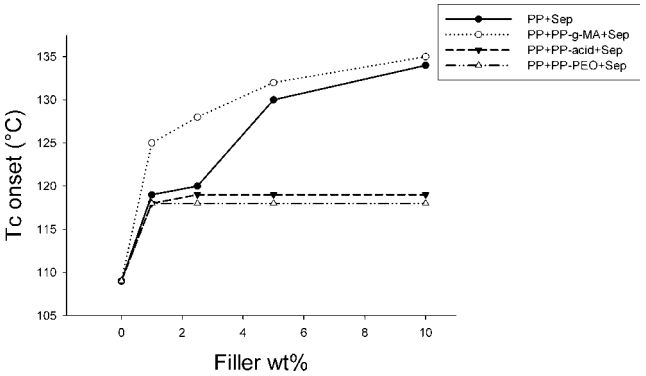

Figure 6 Onset temperatures of starting crystallization with filler concentration. ●, PP+Sep; ○, PP+PP-g-MA+Sep; ▼, PP+PP-acid+Sep; ▲, PP+PP-PEO+Sep. A larger, continuous increase in the crystallization temperature is observed for PP+Sep and PP+PP-g-MA+Sep, while a limiting concentration of crystallization nuclei is reached at 1 wt % of filler for PP+PP-acid+Sep and PP+PP-b-PEO+Sep.

increase in T_c is monotone with filler concentration, significant differences in the action are evident in the different systems. As we can see in Figure 6, the systems with a poor distribution of the nanofibers show the largest and continuous increase in the crystallization temperature while the systems with well dispersed sepiolite show only a small effect and a limiting concentration of crystallization nuclei is reached at 1 wt % of sepiolite, after which no significant changes in T_c are observed. As can be seen from the previous results, there is a substantial difference in crystallization activity between the systems that present a good dispersion of sepiolite in PP and those characterized by agglomeration of the filler.

In general, any filler, including sepiolite, can nucleate PP on its surface or at the connecting lines of two particles.[29,31,32] In our case, the decrease of nucleating efficiency coupled with a better dispersion of the particles seems to be a strong indication for the second mechanism, i.e., that aggregates are the predominant nucleating sites; but there is another possibility as well. Fillers have high-energy surfaces and adsorb

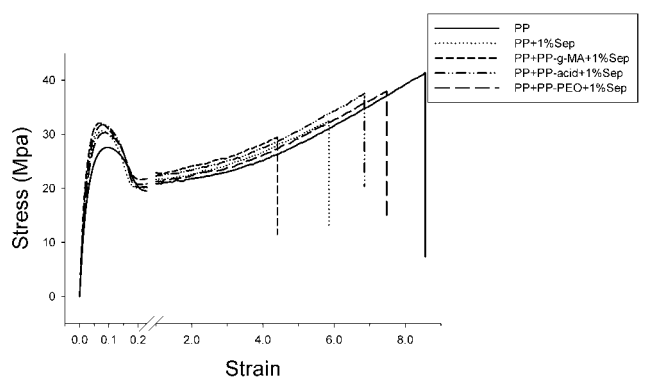

Figure 7 Stress–strain curves of different nanocomposites at a loading of 1 wt % of sepiolite.

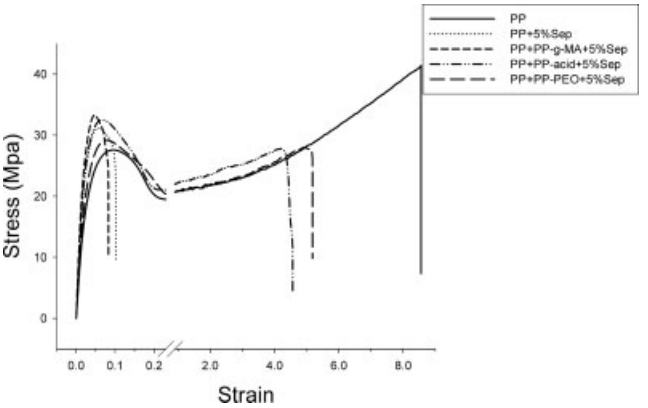

Figure 8 Stress–strain curves of different nanocomposites at a loading of 5 wt % of sepiolite.

the polymer preferentially along their crystal structure. When the filler surface is covered with an organic substance, the surface free energy is decreased, thus also the nucleating efficiency. Moreover, coverage with a thick layer of polymer may change and cover the anisometric topological feature of the filler. The three functionalized polymers are expected to be adsorbed on the filler surface in a specific way. For instance, PP-g-MA has a low degree of functionalization, at least compared with the other two compounds; thus, coverage might be completely different. Moreover, the molecular weight of the PP block in PP-g-MA is much higher than in the case of PP-acid and PP-PEO accounting for a smaller tendency to segregate to the filler surface. Further experiments are under way to study this effect in more detail.

Mechanical properties

The mechanical behavior of the different nanocomposites is displayed in Figures 7 and 8 by representative stress–strain curves. As expected, an increase in Young's modulus is observed for all nanocomposite systems investigated (Fig. 9). More interesting is the

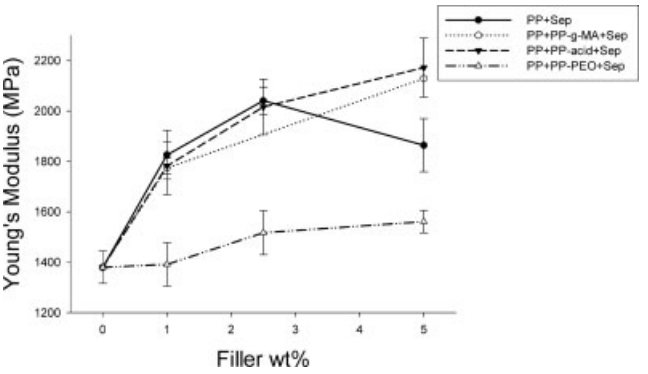

Figure 9 Young's modulus of PP nanocomposites at different filler loadings. A general enhancement with sepiolite content is evident for all the systems.

comparison of the strain to failure for the different systems, as shown in Figure 10. While nanocomposites without functionalized polymers or with PP-g-MA undergo a clear embrittlement at sepiolite concentrations as low as 2.5 wt %, the use of PP-PEO and PP-acid preserves the ductile nature of the polymer matrix, that undergo yielding with necking stabilization and cold drawing, even at filler concentrations of >5 wt %. Only a limited enhancement in yield stress can be noticed in Figure 11. The results of this research underline the promising characteristic of needle-like nanoclay, as reinforcement for thermoplastic polymers. Even better results are expected from reactive surface treatments specifically tailored for Sepiolite. The functionalized polymers employed in this work act as surface-active species and may be classified as nonreactive surface treatments; their main effect is to change interaction between the nanoparticles. Weaker interaction leads to a dramatic decrease in aggregation, improved dispersion, and homogeneity, noted in our study in particular with the use of PP-PEO and PP-acid. However, as an effect of nonreactive treatments, not only particle–particle, but also matrix–particle interaction decreases. The consequence is improved deformability but often decreases yields stress as well as ultimate tensile strength.

CONCLUSION

Three functionalized polymers have been studied and compared in particular for the enhancement of needle-like sepiolite nanoclay dispersion in isotactic polypropylene matrix and mechanical properties. PP-PEO and PP-acid behave more efficiently for PP/Sep nanocomposites compared with the more commonly used PP-g-MA as demonstrated by morphological and mechanical analysis. It is believed that an even better efficiency is possible with a further optimization of the thermodynamics of the surface-active polymers. Furthermore, it was observed that, similar to many other nanofillers, Sepiolite changes the kinetics of crystallization of PP considerably, acting as heterogeneous nuclei and increasing the crystallization temperature. Moreover, although sepiolite did not alter the crystalline structure and crystal polymorphism, it did seem to promote an orientation of the α-phase crystals.

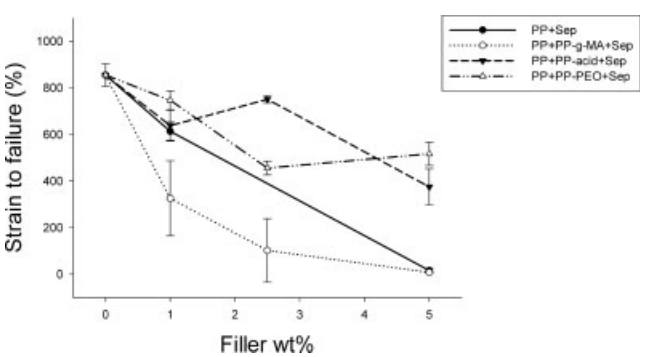

Figure 10 Strain to failure of PP nanocomposites at different filler loadings. While nanocomposites without compatibilizer or with PP-g-MA undergo a clear embrittlement, the use of PP-b-PEO and PP-acid preserves ductility, even at filler concentrations of >5 wt %.

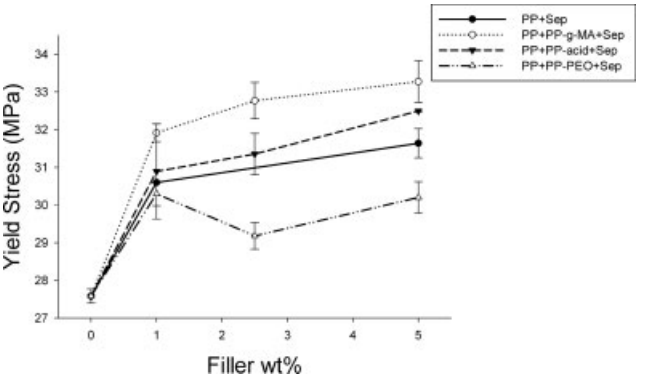

Figure 11 Yield stress of PP nanocomposites at different filler loadings. A limited enhancement of tensile strength with increasing filler content is observed for all nanocomposite formulations.

The authors thank Professor Bela Pukansky for valuable discussions and Tolsa for donating sepiolite clay. We also thank Dr. Zofia Luklinska and Mr. Mick Willis for their help and assistance on SEM and TEM.

References

1. Usuki, A.; Kawasumi, M.; Kojima, Y.; Okada, A.; Kurauchi, T.; Kamigaito, O. J Mater Res 1993, 8, 1174.
2. Giannelis, E. P.; Krishnamoorti, R. K.; Manias, E. Adv Polym Sci 1998, 138, 107.
3. Giannelis, E. P.; Krishnamoorti, R. K.; Manias, E. Adv Polym Sci 1999, 118, 108.
4. Vaia, R. A.; Teukolsky, R. K.; Giannelis, E. P. Chem Mater 1994, 6, 1017.
5. Hackett, E.; Manias, E.; Giannelis, E. P. J Chem Phys 1998, 108, 7410.
6. Alexandre, M.; Dubois, P. Mater Sci Eng 2004, 28, 1.
7. Pinnavaia, T. J.; Beall, T. J. Polymer–Clay Nanocomposites; Wiley: Chichester, UK, 2000.
8. Zanetti, M.; Lomakin, S.; Camino, G. Macromol Mater Eng 2000, 279, 1.
9. Kato, M.; Usuki, A.; Okada, A. J Appl Polym Sci 1997, 66, 1781.
10. Kawasumi, M.; Hasegawa, N.; Kato, M.; Usuki, A.; Okada, A. Macromolecules 1997, 30, 6333.
11. Hasegawa, N.; Kawasumi, M.; Kato, M.; Usuki, A.; Okada, A. J Appl Polym Sci 1998, 67, 87.
12. Reichert, P.; Nitz, H.; Klinke, S.; Brandsch, R.; Thomann, R.; Mulhaupt, R. Macromol Mater Eng 2000, 275, 8.
13. Manias, E.; Touny, A.; Wu, L.; Strawhecker, K.; Lu, B.; Chung, T. C. Chem Mater 2001, 13, 3516.
14. Morales, E.; Ojeda, M. C.; Linares, A.; Acosta, J. E. Polym Eng Sci 1992, 32, 769.
15. Acosta, J. L.; Ojeda, M. C.; Morales, E.; Linares, A. J Appl Polym Sci 1986, 31, 2351.

16. Acosta, J. L.; Ojeda, M. C.; Morales, E.; Linares, A. J Appl Polym Sci 1986, 31, 1869.
17. Van Es, M. Polymer–Clay Nanocomposites. The Importance of Particle Dimensions; PhD thesis; Technical University: Delft, 2001.
18. Grim, R. E. Clay Mineralogy; McGraw-Hill: New York, 1968.
19. Grim, R. E. Applied Clay Mineralogy; McGraw-Hill: New York, 1962.
20. Kuang, W.; Facey, G. A.; Detellier, C. Clays Clay Miner 2004, 52, 635.
21. Fischer, H. Mater Sci Eng 2003, 23, 763.
22. Kudryavtsev, Y. V.; Govorum, E. N.; Litmanovich, A. D.; Fischer, H. R. Macromol Theory Simul 2004, 13, 392.
23. Pukanszky, B. In Polypropylene: Structure, Blends and Composites; Karger-Kocsis, J., Ed.; Chapman & Hall: London, 1995; p 1.
24. Pukanszky, B.; Belina, K.; Rockenbauer, A.; Maurer, F. H. J. Composites 1994, 25, 205.
25. Pukanszky, B.; Mudra, I.; Staniek, P. J Vinyl Additive Technol 1997, 3, 53.
26. Van der Meer, D. W.; Pukanszky, B.; Vancsa, G. J. J Macromol Sci Phys 2002, B41, 1105.
27. Menczel, J.; Varga, J. J Therm Anal 1983, 28, 161.
28. Fujiyama, M.; Wakino, T. J Appl Polym Sci 1991, 42, 2739.
29. Pukanszky, B.; Fekete, E. Polym Polym Compos 1998, 6, 313.
30. Xu, W.; Ge, M.; He, P. J Polym Sci Part B: Polym Phys 2002, 40, 408.
31. Pozsgay, A.; Frater, T.; Papp, L.; Sajo, I.; Pukanszky, B. J Macromol Sci Phys 2002, B41, 1249.
32. Svoboda, P.; Zeng, C. H.; Wang, H.; Lee, J.; Tomasko, D. L. J Appl Polym Sci 2002, 85, 1562.
33. Natta, G.; Corradini, P. Nuovo Cim (Suppl) 1960, 15, 40.
34. Karger-Kocsis, J. Polypropylene Structure, Blends and Composites: Structure and Morphology, Vol. 1; Chapman & Hall: London, 1995.
35. Wang, L.; Sheng, J. Polymer 2005, 46, 6243.
36. Ferrage, E.; Martin, F.; Boudet, A.; Petit, S.; Fourty, G. J Mater Sci 2002, 37, 1561.
37. Rybnikar, F. J App Polym Sci 1989, 38, 1479.